On-chip Testing and Properties of MEMS Materials: Size Scale Effects

1. *Introduction*

Market needs in the micro-electronics industry require the production of devices with increasing performance based on the continuous reduction of the characteristic dimensions of the main components. Therefore, in the last decade many efforts in the scientific community have focused on understanding how the material mechanical behavior changes at small scales, particularly at structural dimensions less than a micrometer. At this small scale the geometric features of the samples become comparable to the characteristic length scales of the material microstructure, and classical plasticity, which is essentially size independent, cannot be applied.

This is especially the case for metallic thin films, which are of particular interest because of their wide use in electronic components. Thin films usually exhibit a flow stress an order of magnitude higher than the same material in bulk form and this flow stress increases as film thickness diminishes (Arzt 1998, Spaepen 2000, Espinosa and Prorok 2001). Several authors investigated the mechanical behavior of thin films on Si substrate; particularly, they focused on the effect of film thickness, grain size, and orientation, on the stress–strain response (Venkatraman and Bravman 1992, Keller *et al*. 1998, Baker *et al*. 2001). Fewer experimental devices are currently available for testing freestanding thin films (Keller *et al*. 1996, Espinosa and Prorok 2001, Haque and Saif 2004). Recently, Espinosa and Prorok (2001), Espinosa *et al*. (2003), and Espinosa *et al*. (2004) developed a new experimental technique, the membrane deflection experiment (MDE), which allowed to test polycrystalline freestanding films such as electron beam evaporated Au, Cu, and Al. Strong size effects were found in the mechanical properties of the films which were polycrystalline in nature with thickness ranging from 200 nm to 1 μm. The average grain size of the samples was $\sim$200 nm and kept constant for all the thicknesses. For the case of electron beam evaporated Cu, similar results were obtained using a microtensile device in Keller *et al*. (1996). Haque and Saif (2004) also investigated the tensile stress–strain response of f.c.c. freestanding metal films such as sputtered pure Al and Au (down to a thickness of 0.1 μm). *In situ* TEM investigations of the samples were also performed and no plastic activity was observed for an average grain size below 50 nm. Therefore, the authors concluded that grain boundary mechanisms were predominant in the deformation process of such materials. However, in such investigation the average grain size was varying with film thickness which does not allow us to isolate the effects of the two characteristic dimensions.

This significant body of experimental results led in the last decade to several modeling efforts toward understanding and interpreting material size scale effects. The purpose of this article is to review and illustrate some new findings from both the experimental and the modeling viewpoints.

2. *Experimental Results*

2.1 *MDE Experiments and TEM/SEM Observations*

As previously mentioned, the MDE is a technique apt to characterize the mechanical behavior of freestanding thin films. The principle of the MDE is recalled in Fig. 1(a): a vertical load (P_V) is applied by a nanoindenter leading to the membrane in-plane load denoted by P_M. The deflection of the membrane Δ is measured independently and the strain in the gauge region of the specimen is measured with a Mirau microscope interferometer. Fig. 1(b) displays the geometry of the tested membranes. More details about the experimental procedure are provided in Espinosa and Prorok (2001) and Espinosa *et al*. (2003, 2004).

Figure 2(a) shows the stress–strain response of electron beam evaporated Au specimens. The plots show that the onset of plasticity was different between membranes with a thickness of 0.3 μm (high yield stress), 0.5 μm and 1.0 μm (low yield stress). A major transition was also observed between 1.0 μm and 0.5 μm, which suggests the existence of different strengthening mechanisms. Similar strong size effects were obtained in the case of electron beam evaporated

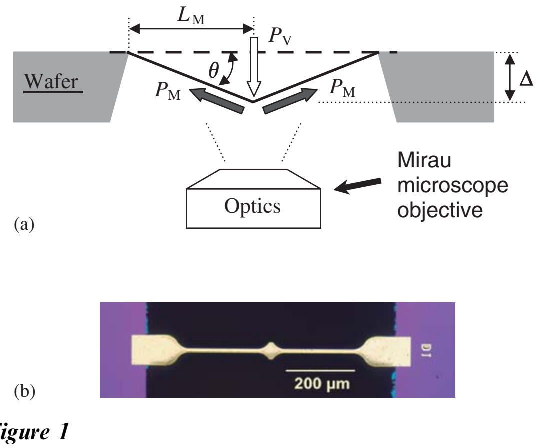

Figure 1
(a) Side view of the MDE test, (b) optical image of an Au membrane (top view) with LM half the membrane span = 200 μm. Reproduced from Espinosa H D, *et al*. 2003 A novel method for measuring elasticity, plasticity and fracture of thin films and MEMS materials. *J. Mech. Phys. Solids* **51**, 47–67, with permission from Elsevier.

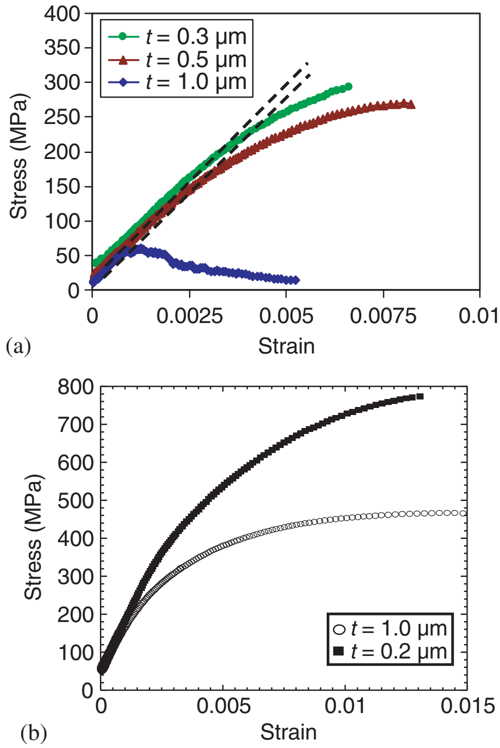

Figure 2
Stress–strain plots describing film thickness effects. (a) Gold (the slope of the dashed line gives an elastic modulus between 53 GPa and 55 GPa), (b) copper (elastic modulus between 125 GPa and 129 GPa). Reproduced from Espinosa H D, *et al.* 2004 Plasticity size effects in free-standing submicron polycrystalline FCC films subjected to pure tension. *J. Mech. Phys. Solids* **52**, 667–89, with permission from Elsevier.

Cu and Al membranes (Fig. 2(b) for the copper case). In order to investigate the nature of these phenomena, post-mortem transmission electron microscopy (TEM) and scanning electron microscopy (SEM) observations on MDE tested films were performed. The samples for TEM observations were prepared following the procedure illustrated in Ishida and Sato (2003). The 0.3-μm-thick Au films presented a smooth surface near the fracture plane which proved the absence of significant plastic activity (Fig. 3(a)). By TEM observations of the same samples, residual dislocation patterns have been found only within a few isolated grains and the dislocation activity was decreasing when departing from the fracture surface. TEM images before testing showed the grains containing annealing twins and basically free of dislocations. On the contrary, SEM images of the 1-μm-thick Au films displayed a more marked plastic activity as evident from the surface roughness of Fig. 3(b). This feature is in agreement with the observed softening of the sample. TEM images of the 1-μm-thick Au films also showed few residual dislocation patterns, which were particularly present in grains with high aspect ratios. This suggests that dislocations were either adsorbed by free surfaces or formed pile-ups at grain boundaries. Therefore, network formation occurred only in grains where the probability of forming dislocation junctions was increased. Our TEM observations are in agreement with the ones reported in Keller *et al.* (1996). In these *in situ* TEM studies, the films exhibited limited plastic activity and dislocations were found to nucleate at grain boundaries with very short glide distances, which did not allow significant dislocation interaction.

2.2 Self-similar Experiments

In order to further investigate the aforementioned plasticity size effects, self-similar experiments have been performed on Cu films. The films were machined out of a copper foil and prepared so that grain size and film thickness were 1000 times larger than the thin films tested by MDE. This implies that the grain boundary area available for defect nucleation was several orders of magnitude larger. The samples were tested in tension with a miniature tensile stage (Fullam, Inc., Latham, NY) equipped with a 2000 lbs load cell. The experiments were observed with an optical microscope and the local strain field was determined through digital image correlation. In Fig. 4 the tensile response of coarse-grained films with thicknesses of 0.3 mm and 1 mm are compared with the ones of thin films with thicknesses of 0.3 μm and 1 μm. As expected, size effect is manifested only in the case of submicron thin films. Figures 5(a) and 5(b) show, respectively, the initial grain structure of the coarse-grained films and the deformed configuration at an applied external strain of ~10%. The main features of the deformation process are the ones of bulk polycrystalline metals where dislocations sweep the grains at relatively low level of deviatoric stress, as evident from the numerous slip lines. In the case of millimeter-thick films, due to the increased grain boundary area and the enlarged probability to find intragranular dislocation sources, defect nucleation does not control anymore the plastic activity. For this reason the macroscopic bulk response is achieved and no significant statistical variations in the sample behavior occur.

3. Modeling of Size Scale Plasticity

Several theories and modeling approaches have been recently proposed to interpret size scale effects. They can be distinguished in two main categories: continuum approaches and discrete approaches. Some of these theories are briefly reviewed in the next section.

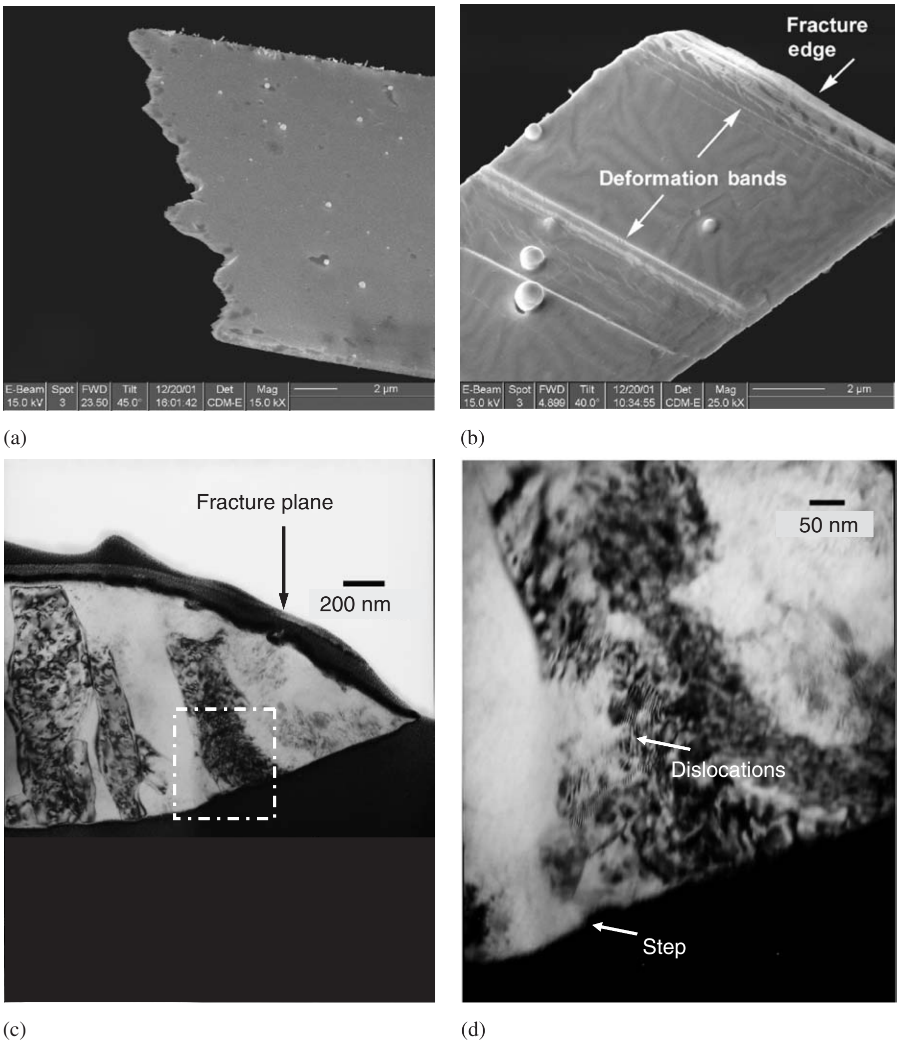

Figure 3
Study of the plastic activity of 0.3-μm-thick Au films. (a) (SEM picture showing the fracture surface) and 1-μm-thick Au films, (b) (SEM picture showing large deformation slip bands close to the fracture edge), (c) cross-sectional TEM view of fracture region, and (d) high aspect ratio grain exhibiting dislocation network. Reproduced from Espinosa H D, *et al*. 2005 Discrete dislocation dynamics to interpret size and grain boundary effects in free-standing FCC thin films. *Int. J. Plast*. (to appear), with permission from Elsevier.

3.1 Continuum versus Discrete Approaches

The first proposed continuum theory was the phenomenological strain gradient plasticity (Fleck and Hutchinson 1997), which was later on improved by the ''mechanism-based'' strain gradient plasticity (Huang *et al*. 2000). These theories attributed size effects to an additional hardening generated by the so-called geometrically necessary dislocations which are required in order to accommodate the gradients of plastic strain. These models have been successfully applied to capture the material behavior for system dimensions ranging from a few microns to 100 μm. However, the aforementioned MDE experiments which are performed in a state of pure macroscopic uniaxial tension prove that further insight is needed to describe thin film plasticity in the submicron range. Recently, Bažant *et al*. (2004) proposed an original continuum approach based on the existence of a boundary layer of fixed thickness produced by the film deposition process on the substrate. The model

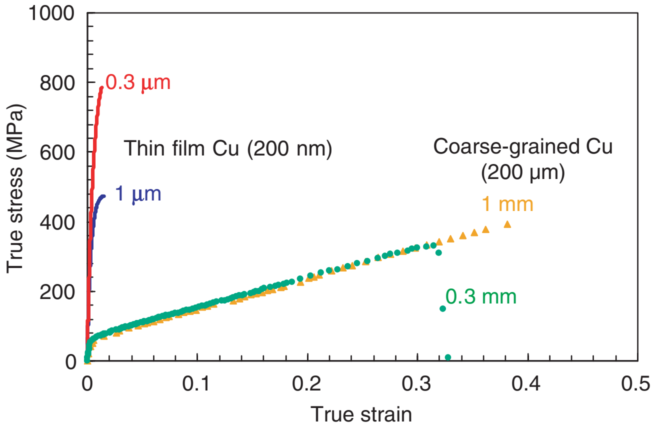

Figure 4
Self-similar experiments in pure tension for Cu films: comparison between the mechanical response of submicronic thin films (MDE) and millimeter thick coarse-grained films (Fullam tensile stage). Reproduced from Espinosa H D, *et al*. 2005 Discrete dislocation dynamics to interpret size and grain boundary effects in free-standing FCC thin films. *Int. J. Plast*. (to appear), with permission from Elsevier.

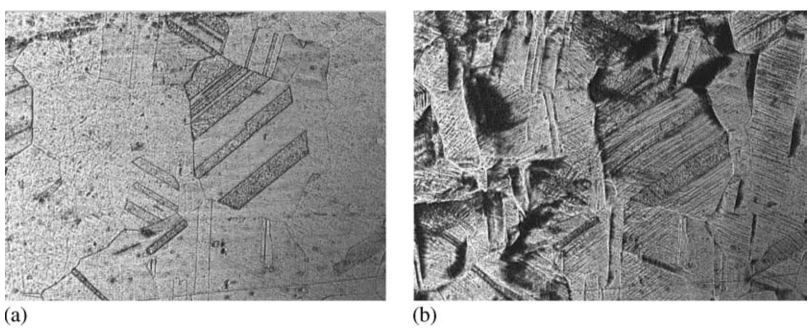

Figure 5
Deformation of coarse-grained films: (a) initial grain structure and (b) grain configuration for an external applied strain of ~10%. Reproduced from Espinosa H D, *et al*. 2005 Discrete dislocation dynamics to interpret size and grain boundary effects in free-standing FCC thin films. *Int. J. Plast*. (to appear), with permission from Elsevier.

was based on a nonuniform distribution of initial yield stress in the thickness due to a gradient of dislocation density in the boundary layer and was able to capture reasonably well the experimental results.

A second different kind of approach is the one based on discrete simulations, like large-scale molecular dynamics or dislocation dynamics. This method is adopted here because emission and evolution of discrete dislocations appear to be a key feature to understand thin film mechanics in the submicronic range. Discrete dislocation dynamics (DDD) proved to be very efficient in the analysis of the influence of defect interaction and self-organization on the material mesoscale constitutive response (Madec *et al*. 2003). Here we summarize the DDD model based on the paranoid code (Schwarz 1999, 2003), which has been employed to analyze the deformation mechanisms leading to the experimentally observed size effects (Espinosa *et al*. 2005). In the next section the fundamentals of the dislocation dynamics scheme are summarized in the framework of the paranoid code. The subsequent section reports the simulation results and their implications.

3.2 Discrete Dislocation Dynamics

Paranoid is a 3D code which discretizes a smooth dislocation line by means of meshing points called nodes. The spacing of the nodes can be reduced down to atomic dimensions, which make the code very suitable to study the evolution of dislocation in confined volumes. The dislocation evolution is obtained by tracking the motion of each meshing node. The local stress tensor is made by three different contributions: the applied external stress, the stress arising from the dislocation themselves, and the stress needed to respect the boundary conditions. From the stress tensor, the Peach–Koehler force may be computed at each node as

$$\underline{\mathbf{f}}_g = (b_i \sigma_{ij} n_j)\underline{\mathbf{n}} \times \underline{\mathbf{dl}} \tag{1}$$

where $\underline{\mathbf{f}}_g$ is the force acting on a dislocation element $\underline{\mathbf{dl}}$ in the glide plane, $\underline{\mathbf{b}}$ is the Burgers vector of the dislocation, $\underline{\mathbf{n}}$ is the unit normal to the glide plane, and $\underline{\boldsymbol{\sigma}}$ is the local stress tensor. Then, each node is moved with a velocity following a simple viscous law:

$$\underline{\mathbf{v}} = \frac{\underline{\mathbf{f}}_g}{B} \tag{2}$$

here B is a phonon viscous drag coefficient. From the evolution of the dislocation configuration at each step, the increment of the average plastic strain tensor may be computed as

$$\overline{\mathrm{d}\varepsilon_{ij}^{\mathrm{p}}} = -\frac{1}{2V}\sum_{k=1}^{N}\left(b_i^{(k)}\mathrm{d}S_j^{(k)} + b_j^{(k)}\mathrm{d}S_i^{(k)}\right) \tag{3}$$

In Eqn. (3) V is the volume of the crystal, N is the number of dislocation segments, and $\mathrm{d}\mathbf{S}^{(k)}$ is the algebraic increment of swept area for the segment k. By applying a computational strain rate to the sample and following the dislocation evolution, with the resulting plastic strain, it is possible to construct the stress versus. strain mesoscale response of the material.

3.3 *Results and Discussion*

Columnar grains representative of the film microstructure have been simulated and the influence of the film thickness on the stress–strain response has been investigated. Therefore, our computational domain was made of a rectangular box with a square base of area d^2 (with d being the grain size: 0.2 μm in the simulations) and a varying height h, representing the thickness of the polycrystalline film. The top and bottom surfaces had attractive character in order to simulate the effect of free surfaces, while the lateral faces of the box were impenetrable to represent the presence of grain boundaries. The axis normal to the film plane was chosen as the $\langle \bar{1}\,\bar{1}\,1 \rangle$-direction in order to match the strong $\langle 111 \rangle$ fiber texture of the tested films. The material employed in the simulations was copper and material parameters along with additional computational details may be found in Espinosa *et al*. (2005).

Samples with four thicknesses have been considered: 0.2 μm, 0.4 μm, 0.6 μm, and 1 μm, while the grain size was constant and equal to 0.2 μm. Thus, the four samples had aspect ratios, respectively, equal to 1, 2, 3, and 5. The dislocation sources were randomly distributed only at grain boundaries in order to represent the effect of grain boundary dislocation sources, which are not of the Frank–Read type in the sense that they do not allow for multiple pile–ups. This is consistent with TEM observations and MD simulations of nanocrystalline samples that, for a grain size of ~200 nm, exhibit a predominance of boundary sources in the plastic process. The sources had a normal distribution of sizes with an average size and a standard deviation, respectively, equal to 0.08 μm and 0.02 μm. The parameters of this distribution were the same for all the thicknesses. Finally, a constant density of sources per unit area of grain boundary ($2.4 \times 10^4\,\mathrm{cm}^{-1}$) was employed.

Three runs for each thickness were performed and the stress–strain results were averaged in order to minimize fluctuations due to the statistical nature of the samples. The four results were compared in Fig. 6 where error bars are reported to represent the statistical scatter at the end of the simulation. The results in Fig. 6 correctly represent the experimentally observed size effects for the thicknesses $h = 0.2$ μm, $h = 0.4$ μm and $h = 0.6$ μm for which thinner is stronger. However, this trend reverses in the case of the 1-μm-thick sample which manifests a hardening rate larger than the 0.6-μm-thick sample. The following interpretation of the aforementioned results is here proposed. Thinner films present less grain boundary area and, consequently, a lower probability to activate boundary

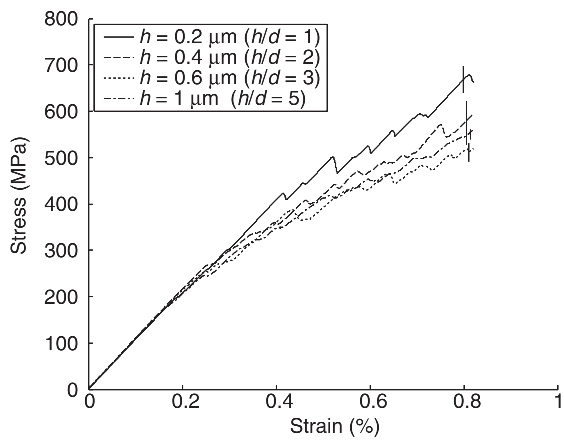

Figure 6
Stress–strain curves for samples with different thicknesses and aspect ratios. Initial grain boundary dislocation density: $2.4 \times 10^4\,\mathrm{cm}^{-1}$. The error bars represent the statistical scatter of different runs at the end of the simulation for each sample. Reproduced from Espinosa H D, *et al*. 2005 Discrete dislocation dynamics to interpret size and grain boundary effects in free-standing FCC thin films. *Int. J. Plast.* (to appear), with permission from Elsevier.

sources at a certain stress level. This is consistent with our self-similar experiments, which do not exhibit any size effect as a consequence of the large grain boundary area available for defect nucleation and the presence of intragranular Frank–Read sources. Moreover, for smaller thicknesses, there is a higher probability for dislocations to encounter free surfaces and to be partially adsorbed; thus, the available free path for dislocations is reduced by the presence of free surfaces and only a limited amount of plastic strain may be produced. However, the effect of these two features is disappearing when the film thickness and the grain aspect ratio are increasing. In fact, for larger aspect ratios ($h = 1\,\mu m$, $h/d = 5$), the probability for dislocations to pile up at grain boundaries and intersect each other by forming networks and junctions is higher. This characteristic has been called "aspect ratio effect" and analyzed in detail in Espinosa *et al.*

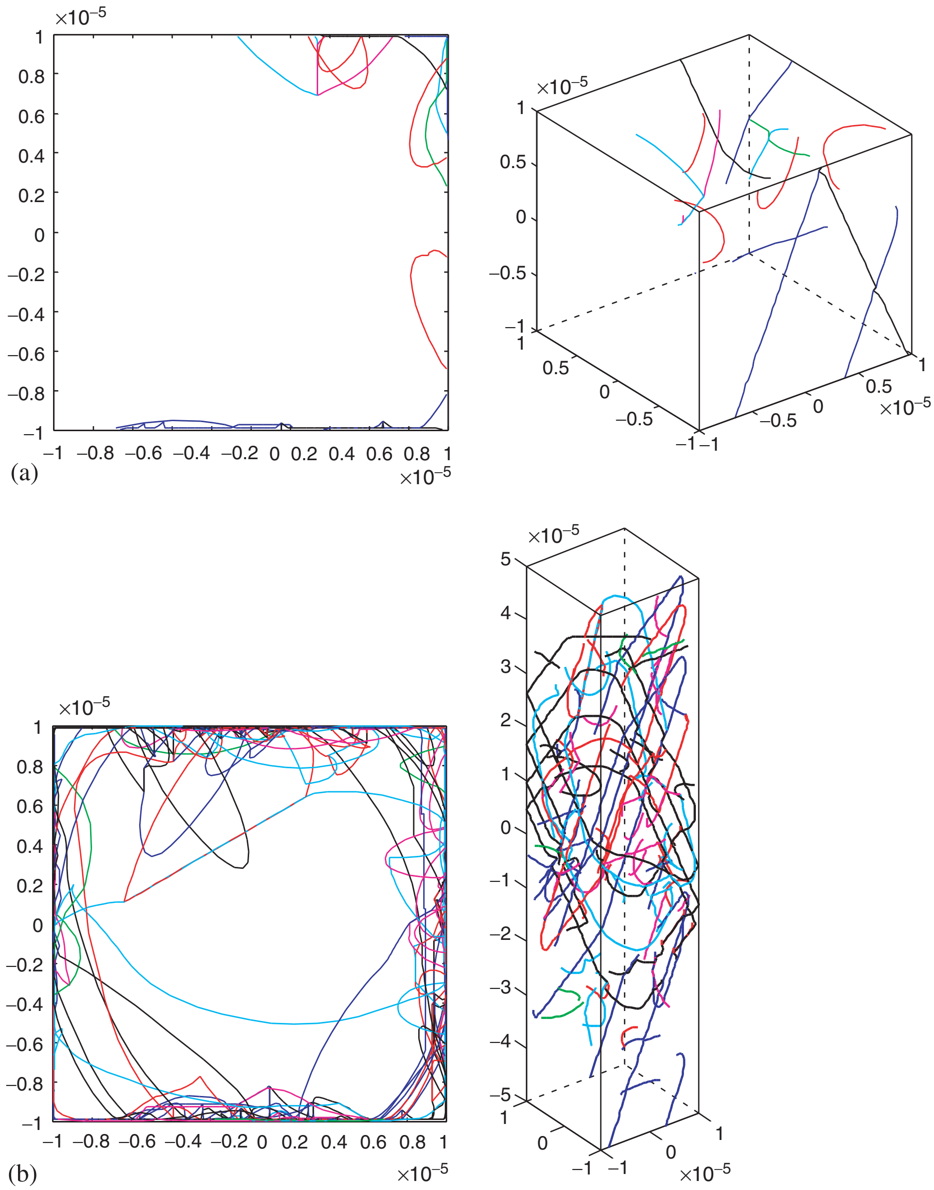

Figure 7
Final dislocation configurations for an applied strain of 0.8% (left images: top view, right images: 3D view): (a) 0.2 μm sample and (b) 1 μm sample.

(2005); it generates an increase of the internal stress (back stress) during the deformation process; this causes an obstacle to further dislocation nucleation, leading to an increase in hardening rate. Figure. 7 shows snapshots of the dislocation structure for an applied strain of 0.8% and two different samples (0.2 μm and 1 μm; only active dislocation sources are plotted). These snapshots show the formation of junctions only in the 1-μm-thick sample. This is consistent with our TEM observations (Fig. 3(d)) which present evidence of networks formation only in the grains with highest aspect ratio. It should be mentioned that the size effect saturation above described is a function of the density of sources as explained in Espinosa *et al.* (2005).

4. Conclusion and Future Challenges

In this work some new experimental and numerical findings on the plasticity size scale effects have been reported. A DDD model has been proposed based on the assumption that sources are scarcely available in geometrically confined volumes and that the most probable nucleation sites are at grain boundaries. These hypotheses have been supported by TEM investigations of the tested samples, which show the grains initially free of defects with residual dislocation networks only in the highest aspect ratio grains. Self-similar experiments were also performed in order to support the idea that in submicron thin films the deformation process is controlled by nucleation of defects.

By simulating columnar grains representative of the film microstructure and changing the film thickness and, hence, the available surface for dislocation nucleation, we were able to capture qualitatively the same trend than the experimentally observed size effects. This effect was gradually saturating for increasing aspect ratios of the columnar grain, due to the increase in internal stresses generated by junction formation and pile-up at the impenetrable boundaries. We have shown that the approach here adopted is able to capture the essential features of the discrete mechanisms involved. However, assumptions were required in order to simplify the computational problem. For instance, we have assumed a density of sources distributed at grain boundaries with sizes randomly generated by means of a normal distribution. This starting configuration can only qualitatively represent the real nature and complexity of a grain boundary. This structure, at least for low-angle grain boundaries, can be seen as arrays of dislocations which under an appropriate stress condition may be pulled out and propagate into the interior of the grain. On the other hand, grain boundaries have also manifested at a certain extent the ability to adsorb dislocations, which enter the boundary by modifying its atomic structure. This emission–adsorption process requires a deeper modeling effort where atomistic simulations are likely to improve our knowledge of modifications in the grain boundary structure and to formulate an energetic activation criterion to be incorporated in DDD.

Bibliography

Arzt E 1998 Size effects in materials due to microstructural and dimensional constraints: a comparative review. *Acta Mater.* **46**, 5611–26

Baker S P, Kretschmann A, Arzt E 2001 Thermomechanical behavior of different texture components in Cu thin films. *Acta Mater.* **49**, 2145–60

Bažant Z P, Guo Z, Espinosa H D, Zhu Y, Peng B 2004 Epitaxially influenced boundary layer model for size effect in thin metallic films. *J. Appl. Phys.* **97**, 073506

Espinosa H D, Prorok B C 2001 Effects of film thickness on the yielding behavior of polycrystalline gold films. *Mater. Res. Soc. Symp. Proc.* **695**, L8.3.1–6

Espinosa H D, Prorok B C, Fischer M 2003 A novel method for measuring elasticity, plasticity and fracture of thin films and MEMS materials. *J. Mech. Phys. Solids* **51**, 47–67

Espinosa H D, Prorok B C, Peng B 2004 Plasticity size effects in free-standing submicron polycrystalline FCC films subjected to pure tension. *J. Mech. Phys. Solids* **52**, 667–89

Espinosa H D, Panico M, Berbenni S, Schwarz K W, 2005 Discrete dislocation dynamics to interpret size and grain boundary effects in free-standing FCC thin films. *Int. J. Plast.* (to appear)

Fleck N A, Hutchinson J W 1997 Strain gradient plasticity. *Adv. Appl. Mech.* **33**, 295–361

Haque M A, Saif M T A 2004 Deformation mechanisms in free-standing nanoscale thin films: a quantitative *in situ* transmission electron microscope study. *Proc. Nat. Acad. Sci. USA* **101**(17), 6335–40

Huang Y, Gao H, Nix W D, Hutchinson J W 2000 Mechanism-based strain gradient plasticity-II. Analysis. *J. Mech. Phys. Solids* **48**, 99–128

Ishida A, Sato M 2003 Thickness effect on shape memory behavior of Ti–50.0at.%Ni thin film. *Acta Mater.* **51**, 5571–8

Keller R R, Phelps J M, Read D T 1996 Tensile and fracture behavior of free-standing copper films. *Mater. Sci. Eng.* **A214**, 42–52

Keller R M, Baker S P, Arzt E 1998 Quantitative analysis of strengthening mechanisms in thin Cu films: effects of film thickness, grain size, and passivation. *J. Mater. Res.* **13**(5), 1307–17

Madec R, Devincre B, Kubin L, Hoc T, Rodney D 2003 The role of collinear interaction in dislocation-induced hardening. *Science* **301**, 1879–82

Schwarz K W 1999 Simulation of dislocations on the mesoscopic scale. I: methods and examples. *J. Appl. Phys.* **85**(1), 108–19

Schwarz K W 2003 Local rules for approximating strong dislocation interactions in discrete dislocation dynamics. *Model. Simul. Mater. Sci. Eng.* **11**, 609–25

Spaepen F 2000 Interfaces and stresses in thin films. *Acta Mater.* **48**, 31–42

Venkatraman R, Bravman J C 1992 Separation of film thickness and grain-boundary strengthening effects in Al thin-films on Si. *J. Mater. Res.* **7**(8), 2040–8

H. D. Espinosa, S. Berbenni, M. Panico, and B. Peng

Encyclopedia of Materials: Science and Technology
ISBN: 0-08-043152-6
pp. 1–8